Carbon 116 (2017) 695–702

Contents lists available at ScienceDirect

Carbon

journal homepage: www.elsevier.com/locate/carbon

One-step exfoliation and functionalization of graphene by hydrophobin for high performance water molecular sensing

Jin Tao [a, g, 1], Yanyan Wang [a, 1], Yunjie Xiao [c, d], Pei Yao [e], Cheng Chen [b], Daihua Zhang [a], Wei Pang [a], Haitao Yang [b], Dong Sun [f], Zefang Wang [b, c, d, *], Jing Liu [a, **]

[a] State Key Laboratory of Precision Measurement Technology and Instruments, School of Precision Instruments and Opto-electronics Engineering, Tianjin University, NO.92 Weijin Road, Tianjin 300072, People's Republic of China
[b] School of Life Sciences, Tianjin University, NO.92 Weijin Road, Tianjin 300072, People's Republic of China
[c] State Key Laboratory of Medicinal Chemical Biology, College of Pharmacy, Nankai University, NO.94 Weijin Road, Tianjin 300071, People's Republic of China
[d] Tianjin International Joint Academy of Biotechnology and Medicine, NO.220 Dongting Road, Tianjin 300457, People's Republic of China
[e] School of Materials Science and Engineering, Tianjin University, NO.92 Weijin Road, Tianjin 300072, People's Republic of China
[f] International Center for Quantum Materials, School of Physics, Peking University, NO.5 Yiheyuan Road, Beijing 100871, People's Republic of China
[g] Changchun Institute of Optics and Fine Mechanics and Physics, Chines Academy of Science, NO.3888 Nanhu Road, Changchun 130033, People's Republic of China

ARTICLE INFO

Article history:
Received 6 October 2016
Received in revised form
4 February 2017
Accepted 17 February 2017
Available online 20 February 2017

ABSTRACT

A novel one-step strategy to exfoliate and functionalize two dimensional layered materials (2DLM) is described to promote the production and performance of the 2DLM for bio-related and molecule adsorption based practical applications. This method applies sonication to the 2DLM dissolved in the aqueous solution of hydrophobin protein, during which process the hydrophobins penetrate into the interlayer and automatically bind onto the surface of 2DLM to peel off the mono-/few-layer from the bulk material. The exfoliated 2DLM is spontaneously wrapped with a dense and ordered hydrophobin monolayer, forming unique bio-nanocomposites with greatly enhanced biocompatibility and molecule adsorption capability. The product exfoliated and functionalized by this method from reduced graphite oxide is successfully applied for an exemplary application of water molecular sensing, which, to the best of our knowledge, is the first time that a protein layer is used as an active sensing layer for water molecules. The device shows exceptional improved performance in harsh environments with complicated background interferents as compared to a bare reduced graphene oxide sensor and a commercial sensor.

1. Introduction

With tremendous research advances in two dimensional layered materials (2DLM) since the discovery of graphene in 2004 [1], both on unique fundamental properties and enormous prototype demonstrations of supreme applications [2–4], the mass production of few-layer 2DLM at large-scale and its functionalization for certain applications, especially those for bio compatible applications, remain challenge in the community. Previously, tremendous efforts have been made in large-scale liquid phase exfoliation of 2DLM from its bulk counterpart with various solvents [5–8] and then functionalize it with chemicals [9–11], bio-molecules [12] and nanoparticles [13,14] to achieve stable dispersion of 2DLM in solution [15,16] and/or designed properties of the final composites [9–14]. These two-step methods are not only time-consuming [17], but also require careful selection of the solvents used in the two sequential processes to prevent any undesired reactions or pollution caused by the interferents from the previous step, which may degrade the function of the final products [18]. Therefore, new strategies, especially one-step exfoliation and functionalization, are

* Corresponding author. School of Life Sciences, Tianjin University, NO.92 Weijin Road, Tianjin 300072, People's Republic of China.
** Corresponding author. School of Precision Instruments and Opto-electronics Engineering, Tianjin University, NO. 92 Weijin Road, Tianjin 300072, People's Republic of China.
E-mail addresses: zefangwang@tju.edu.cn (Z. Wang), jingliu_1112@tju.edu.cn (J. Liu).
[1] These authors contributed equally to this work.

http://dx.doi.org/10.1016/j.carbon.2017.02.052
0008-6223/

highly desired for exploiting 2DLM in large-scale practical applications.

For this purpose, chemistry approaches to liquid exfoliate and functionalize 2DLM have been extensively studied in previously works [19–21], however, potential solutions from life science are appealing but less explored [22–24] so far. Protein, as the main bearer of abundant life activities, if feasible, provides obvious advantages for this purpose due to its excellent bio-compatibility. Hydrophobin, used in this work, is a protein family secreted by fungal that can self-assemble onto various hydrophobic/hydrophilic interfaces to form a very stable and robust protein film with a well ordered pattern [25–27]. The foundation for the self-assembly of hydrophobin is its unique amphiphilic protein structure with a large "hydrophobic patch" on its surface, which can directly interact and bind with hydrophobic materials [28–30]. Thus, hydrophobin can enter the interlayer gap of the 2DLM and automatically bind its hydrophobic patch onto the hydrophobic surface of 2DLM to peel off mono-/few-layer from the bulk counterpart during sonication. At the same time, the peeled off 2DLM is wrapped with a monolayer hydrophobin forming a bio-nanocomposite.

In this work, we demonstrate that large-scale liquid exfoliation and functionalization of 2DLM can be achieved in a single step process by the hydrophobin (HFBI) protein. This one-step method applies sonication to the 2DLM dissolved in the aqueous solution of hydrophobin protein and the exfoliated 2DLM is spontaneously wrapped by a dense and ordered hydrophobin monolayer. This novel strategy appreciably promotes the production and performance of the 2DLM for biomedical related and molecule adsorption based practical applications, due to the hydrophobin functionalization introduced biocompatibility and surface affinity. The product exfoliated and functionalized by this method from reduced graphite oxide is successfully applied for an exemplary application of water molecular sensing, which to the best of our knowledge is the first time that a protein layer is used as an active sensing layer for water molecules, the most essential element for life. The fabricated sensor shows exceptional improved performance in harsh environments with the disturbance of background volatile organic compounds (VOCs) and large pH variations as compared to bare reduced graphene oxide (rGO) sensor and a commercial sensor.

2. Experimental

2.1. Preparation of HFBI wrapped rGO

The HFBI solution was prepared by dissolving 0.20 mg HFBI into 1 mL phosphate buffers (pH value is 7.2). One milligram of reduced graphene oxide (*Timesnano, NO: THRGO, Chengdu, China,* diameter: 0.5–3 mm, thickness: 0.55–3.74 nm) was dissolved in 1 mL of the prepared HFBI solution and the mixture was ultra-sonicated for 30 min. Then air was introduced into the solution for 10 min to remove the remnant HFBI and the solution was ultra-centrifuged for 20 min at 8000 rpm. After these procedures, the supernatant was formed on top of the solution. Top 80% of the supernatant containing HFBI wrapped rGO was collected and lyophilized for further analysis. The concentration of HFBI wrapped rGO flakes was estimated to be 1 mg/mL by measuring the mass of lyophilized powder of the top 80% supernatant after centrifugation.

2.2. Pendant drop experiment

The water solution of HFBI with the concentration of 0.2 mg/mL was continuously pushed out of a syringe needle at a constant speed for 7 s to form an 8 mL pendant drop. After keeping this volume for 1 s, the solution was pulled back into the syringe needle at a constant speed for 4 s. The animation of the pendant drop shape was recorded by a KSV Cam200 goniometer (KSV Instruments) at 66 ms intervals.

2.3. Characterization of HFBI wrapped rGO flakes

Fourier-transform infrared (FT-IR) spectra were performed with a *BRUKER* IFS 55 FTIR system. Raman spectra were acquired with a DXR Microscopy (*Thermo Scientific, USA*) with a 532 nm laser. For both experiments, the HFBI wrapped rGO flake was drop casted onto Si/SiO_2 substrate and washed by DI water, while the sample of bare rGO was freshly exfoliated from reduced graphite oxide and also transferred onto Si/SiO_2 substrate. Atomic force microscopy (AFM) measurements were performed using a Dimension Icon (*Bruker, German*) instrument running in tapping mode. The AFM samples were prepared by drop casting the HFBI wrapped rGO solution on the Si/SiO_2 substrate. High-resolution transmission electron microscopy (HRTEM) images were taken with a Tecnai G2 F20 (*FEI, USA*), operated at 200 kV to visualize the interface of HFBI/rGO. HRTEM samples were prepared by pipetting several microliters of HFBI wrapped rGO solution onto the holey carbon grid.

2.4. Humidity sensor fabrication

The manufacture process of the humidity sensors was as follows: first, the comb electrode was deposited on the Si/SiO_2 substrate by the standard lift-off process. The size of the whole electrode was 1×1.5 mm. The width and length of each electrode finger were 10 μm and 350 μm, respectively, with a lateral spacing of 10 μm. Then 1 μL droplet of aqueous solution of HFBI wrapped rGO flakes was casted onto the comb electrode by a micropipette. When the solvent was evaporated, a thin film of HFBI wrapped rGO flakes was formed at the top of the electrode. The device was then rinsed with pure water to remove the solvent residues and dried by nitrogen flow. At last, the device was attached to a testing board and wire bonded for further testing.

The bare rGO sensor was prepared by the same processes as the HFBI wrapped rGO sensor, except that the liquid exfoliation was carried out by the organic solvent *N*-methyl-pyrrolidone (NMP).

2.5. Sensing setup

The humidity sensing setup contained two parts: the water vapor delivering and electrical testing. The testing chamber was made by a PVC syringe head with a volume of 5 mL which encapsulates the testing board where the HFBI wrapped rGO sensor was attached to. There were several holes drilled through the testing board to vent the water vapor to keep a constant atmospheric pressure. The water vapor was delivered into the testing chamber by bubbling N_2 (99.999%) through a bubbler filled with water. Various concentrations of water vapor were achieved by adjusting the flow velocity ratio between the carrier N_2 and dilution N_2 which was directly connected to the testing chamber. The flow velocity was controlled and monitored by MFCs (NO. 5850e, *Brooks*, *USA*) and the flow meter (Model: red-y, *Vögtlin, Swiss*), respectively, to investigate water vapor concentration dependent response of the HFBI wrapped rGO sensor. Regarding to the electrical testing part, a *Keithley* sourcemeter (NO. 2636) was connected to the testing board through coaxial to measure the electrical signals. A computer was used to control the *Keithley* sourcemeter and MFCs and collect sensing data through GPIB.

During experiments, the RH of the chamber was kept at 0% by inflating pure nitrogen gas through the chamber, and then the RH was changed to a predetermined value by inflating water vapor through and kept at this value for a predetermined period, after which it was turned back to 0% again.

The VOCs detection was conducted by individually delivering each VOC into the testing chamber by bubbling nitrogen through its liquid phase counterpart with the partial pressure of $P/P_0 = 0.3$.

3. Results and discussion

3.1. Hydrophobin HFBI can self-assemble into a protein film with high mechanical strength and flexibility

The mechanical strength and flexibility of HFBI are demonstrated by the pendant drop experiment as shown in Fig. 1a. At the beginning (Fig. 1a I) the HFBI solution drop has a round shape

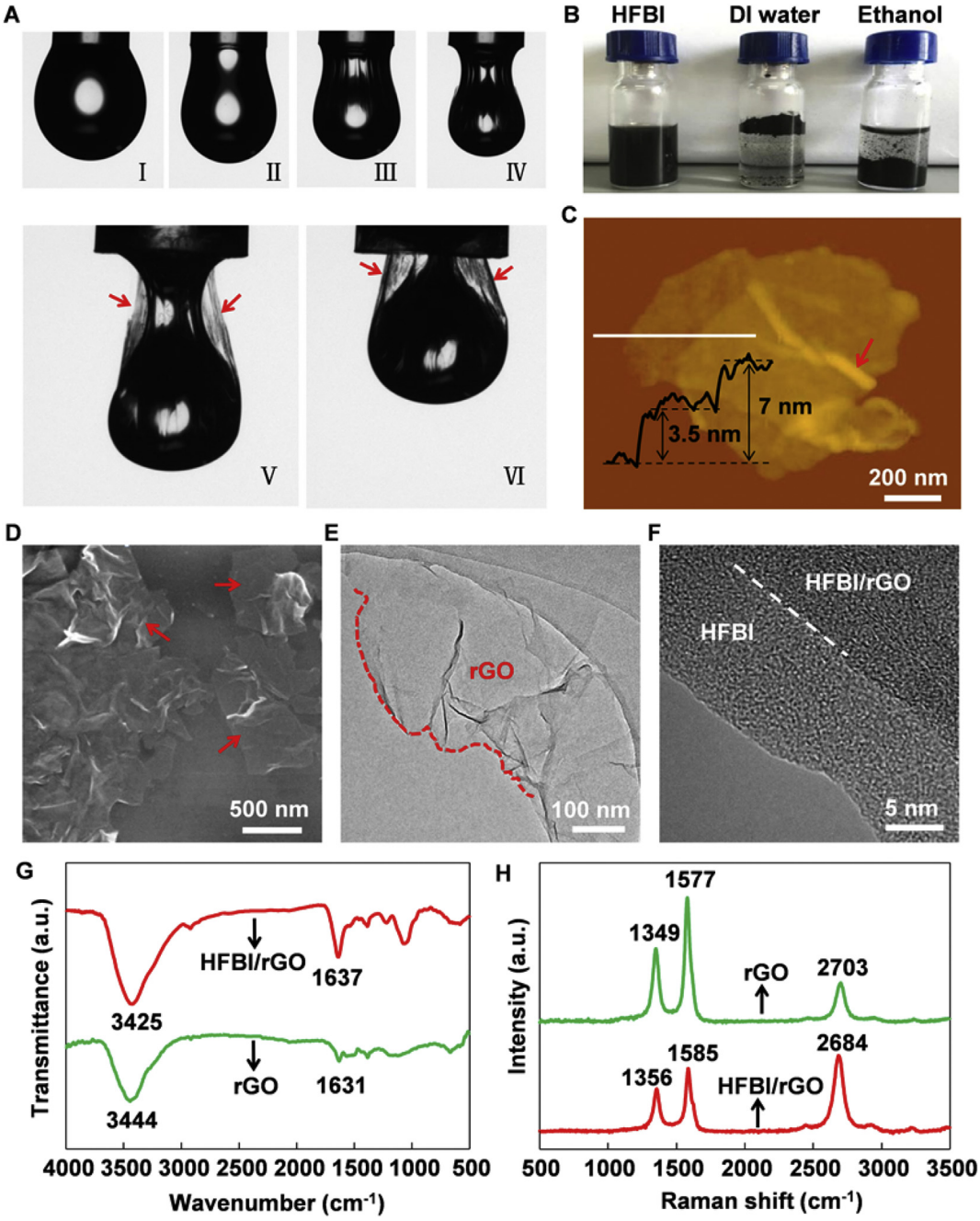

Fig. 1. Characterization of the self-assembly HFBI film and the rGO flake exfoliated and functionalized by HFBI. (a) Pendant HFBI solution drop profiles. The drop shrank gradually and the HFBI film was formed at the surface of the drop. (b) Photograph of the rGO dispersions in 0.2 mg/mL HFBI solution, pure DI water and ethanol, respectively. (c) AFM image of two HFBI wrapped rGO flakes stack together on the substrate. The thicknesses of one- and two-layered HFBI wrapped rGO flakes are around 3.5 nm and 7 nm, respectively. The wrinkle marked with a red arrow indicates the film-structured HFBI wrapped rGO flake. SEM (d), TEM (e) and HRTEM (f) images of the HFBI wrapped rGO flakes on the substrate, respectively. FT-IR spectra (g) and Raman spectra (h) of bare rGO and HFBI wrapped rGO, respectively. (A colour version of this figure can be viewed online.)

similar to that of a water drop, then the HFBI solution drop begins to shrink continuously and the shape changes (Fig. 1a II-IV). When its volume decreases to a certain threshold, the HFBI solution drop has a wrinkled film wrapping outside as indicated by the red arrows (Fig. 1a V-VI). This indicates that the HFBI in the solution travelled towards the vapor-liquid interface and gradually self-assembled into a protein film which holds the droplet from falling down.

3.2. Mass production of mono-/few-layered rGO by liquid exfoliation with hydrophobin HFBI solution

Fig. 1b shows the exfoliation results of sonicating reduced graphite oxide in three solutions: 200 μg/mL HFBI solution, pure DI water and ethanol (from left to right), respectively. Only the one processed with 200 μg/mL HFBI solution had a uniformly black color which stayed unchanged even after three months, suggesting a stable and uniform dispersion of exfoliated rGO flakes in the liquid. In contrast, the other two solutions were transparent with a large amount of bulk reduced graphite oxide powder either floating on the surface or precipitating at the bottom, indicating poor exfoliation effects.

Then a droplet of the HFBI exfoliated rGO solution was sprayed on the silicon substrate for further characterizations. Fig. 1c is the AFM image of two HFBI wrapped rGO flakes stacked together. Line profile as shown in the inset of Fig. 1c is measured along the white line, from which the thickness of the HFBI wrapped rGO flake is identified to be 3.5 nm. This thickness is consistent with the thickness of naked HFBI that is measured in the previous reported results [28]. For this reason, we infer the as measured exfoliated rGO flake is a monolayer. We further measured the thickness of 32 exfoliated sample flakes by AFM which shows that the percentage of monolayer, bilayer and few-layer flakes were 31.2%, 18.8% and 50.0%, respectively (shown in Fig. 1S(A) and (B)). The SEM image (Fig. 1d) shows that the size of exfoliated rGO flake is around 500 × 900 nm with the wrinkling paper-like structure. In low resolution TEM image (Fig. 1e), an exfoliated HFBI wrapped rGO flake is identified according to color contrast to the substrate as labeled with "rGO". High resolution TEM image (Fig. 1f) resolves the

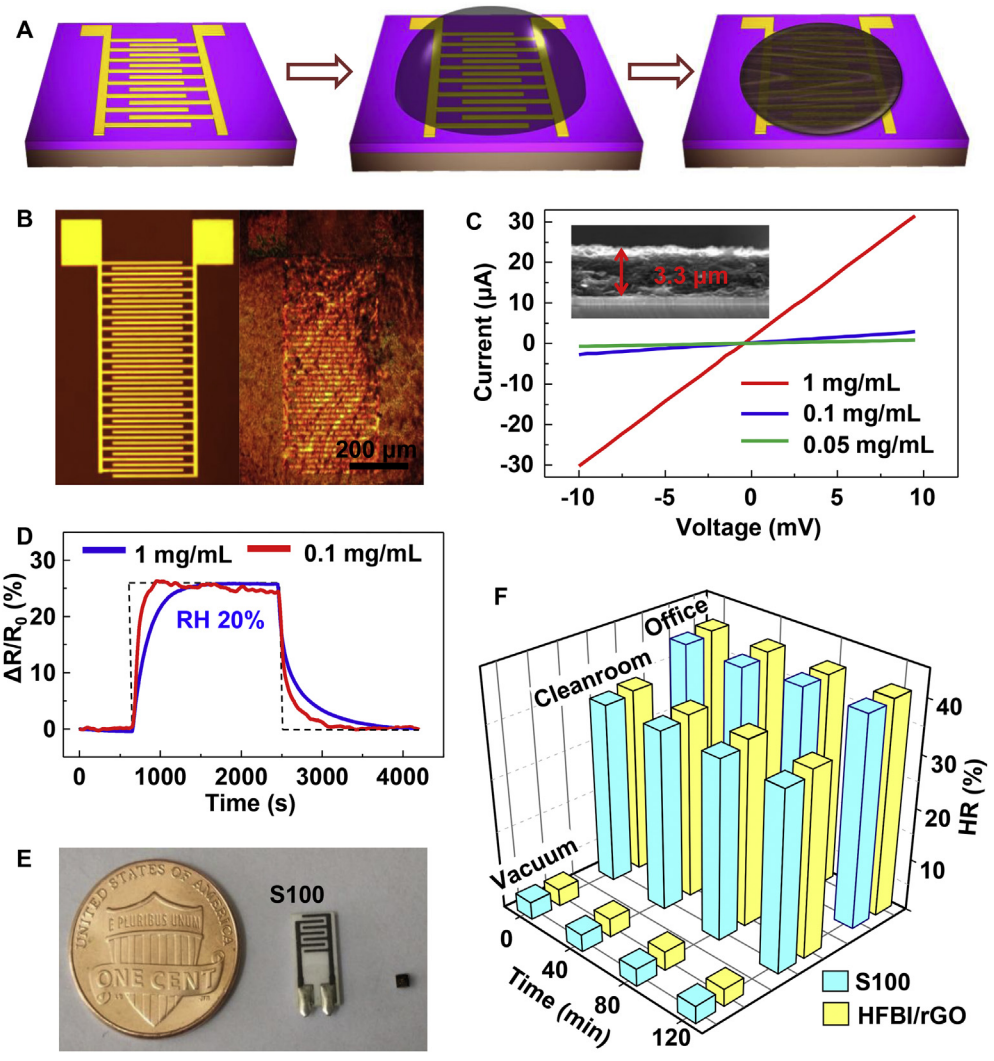

Fig. 2. (a) Fabrication process of the HFBI wrapped rGO sensor. (b) Optical images of the comb electrode before and after coating a layer of HFBI wrapped rGO flakes. (c) I-V curves of the HFBI wrapped rGO sensors made with different concentrations, which correspond to the film thicknesses/resistances of 3.4 μm/0.33 kΩ, 2.0 μm/3.66 kΩ and 0.82 μm/13.04 kΩ, respectively. Inset is the SEM image of the cross-section of the HFBI wrapped rGO film. (d) Real time responses of two HFBI wrapped rGO sensors to 20% relative humidity changes, which were made by two solutions with concentrations of 1 mg/mL and 0.1 mg/mL, respectively. The response/recovery times were 360/470 s and 130/200 s for sensors made of 1 mg/mL and 0.1 mg/mL solutions, respectively. (e) Picture of a one-cent coin, HFBI wrapped rGO sensor and a commercial sensor S100 (from left to right). (f) Sensing results of the HFBI wrapped rGO sensor and S100 sensor in vacuum environment, a 100 class cleanroom and student office over 2 h. (A colour version of this figure can be viewed online.)

interfaces between rGO/HFBI and HFBI/substrate, demonstrating the exfoliated rGO is wrapped by HFBI film.

To further confirm the functionalization of rGO with HFBI, the absorption spectra were performed to characterize the HFBI exfoliated rGO in comparison with mechanically exfoliated bare rGO. As shown in Fig. 1g, both samples have absorption peaks at around 3400 cm^{-1} in the absorption spectra, which is attributed to the O–H stretching vibrations in water solution [31,32]. The presence of a peak at 1630 cm^{-1} is related to the characteristic C=C bond of graphene [33]. However, only HFBI functionalized rGO has the absorption peak at 1637 cm^{-1}, which corresponds to the amide I band of HFBI [32], indicating that the HFBI is dominated by beta-sheet structure when covering the rGO surface. This result is quite consistent with the previous reports that class II hydrophobin formed beta-sheet structure when they assembled physically onto a hydrophobic surface. It verifies the hypothesis that noncovalent hydrophobic interaction between the hydrophobic part of HFBI and rGO is the major driving force for the formation of HFBI wrapped rGO flake [32,34,35].

In Fig. 1h, the Raman spectra of the HFBI exfoliated rGO and mechanically exfoliated bare rGO are compared. Both samples show D, G and 2D Raman modes which are attributed to rGO, demonstrating that the HFBI does not affect the lattice structure of the rGO. Moreover, we can infer the as measured rGO is monolayer from an intensity ratio of 0.5 between the 2D and G peaks of the HFBI wrapped rGO [36]. On the other hand, the relatively high intensity ratio between D and G peak compared to bare rGO suggests more defects exist in HFBI exfoliated rGO samples [37,38]. This is probably because the size of HFBI exfoliated sample is relatively smaller (~100 nm) compared to mechanically exfoliated bare rGO sample (~μm), resulting in increased perimeter to area ratio and more edge associated defects.

3.3. HFBI wrapped rGO flake for water molecular sensing

The HFBI wrapped rGO flakes were used for water molecular sensing as an exemplary application. Fig. 2a shows the fabrication process of the sensor: firstly, a comb electrode is patterned on the Si/SiO_2 substrate; then the solution of HFBI wrapped rGO flakes is drop coated on the electrode and subsequently dried under ambient air to form a uniform film for further sensing test. Fig. 2b is the optical microscope images of the electrode before and after drop coating the HFBI wrapped rGO flakes, respectively. It can be seen clearly that a layer of HFBI wrapped rGO flakes was coated on the electrode surface.

The electrical property of the HFBI wrapped rGO sensor was tested by *I–V* measurement, as shown in Fig. 2c. The *I–V* curves of the HFBI wrapped rGO devices from three solutions with different concentrations were recorded, which shows that the sensor prepared by the HFBI wrapped rGO solution with a higher concentration result in thicker film and thus better conductivity than the one prepared by a lower concentration (Inset of Fig. 2c presents the SEM image of the cross section of the HFBI wrapped rGO film made by 1 mg/mL solution.). Fig. 2d shows the response time depends strongly on the concentration of the HFBI wrapped rGO solution, and consequently the thickness of the film that is formed. As the film thickness decreases from 3.4 μm (for 1 mg/mL solution) to 2 μm (for 0.1 mg/mL solution), the sensor respond/recovery times shorten from 360/470 s to 130/200 s, which is comparable with the humidity sensors reported in Refs. [39–41]. This is due to that water molecules take longer time to penetrate into the thick layers of HFBI wrapped rGO flakes than into thin layers. Therefore, by further thinning the film thickness down to tens of nanometers, its response/recovery times can be potentially comparable with the humidity sensors reported in Refs. [42–44]. Fig. 2e compares the size of HFBI wrapped rGO hybrid sensor with a coin and a commercially available sensor marked as “S100”, exhibiting its miniaturized size. While Fig. 2f demonstrates its comparable stability with “S100” when both of them were placed under three different working environments of vacuum, clean-room and office for 2 h, respectively.

Fig. 3 compares the real-time responses of the HFBI wrapped rGO and bare rGO based sensors to various relative humidity (RH) ranging from 2% to 50%. The results show that the HFBI wrapped rGO sensor has a sensitivity of around 2.24 times resistance change per RH, which is 27 times improvement over bare rGO sensor (0.083 times resistance change per RH). It demonstrates that the sensing capability of HFBI wrapped rGO to water molecules is greatly enhanced compared to bare rGO, indicating fabulous adsorption capacity of HFBI protein to water molecules. The sensitivity of the HFBI wrapped rGO sensor is also higher than the humidity sensors made of bare graphene [42] and rGO/polymer nanocomposites [40], respectively, which again demonstrates its high water uptake capability. Although its sensitivity is lower than the one reported by Ali and co-workers [44], the HFBI wrapped rGO sensor shows great stability and selectivity in complex environments.

Due to the stability and adsorption selectivity of HFBI, the HFBI wrapped rGO sensor can be used for water molecular sensing in environments with complicated background interferents. To demonstrate this, three VOCs (ethanol, acetone and hexane) were used to test the selectivity of the HFBI wrapped rGO sensor to water vapor. As shown in Fig. 4a, the sensor shows the largest response to water vapor, which is approximately one order of magnitude higher than all other three gases, demonstrating an excellent selectivity to water molecules. Additionally, the sensor has larger response to polar VOCs of ethanol and acetone comparing to non-polar VOC of hexane. We speculate the selectivity to water molecules is due to the fact that the hydrophilic part of HFBI prefers to absorb water molecules than other gas molecules. Moreover, the hydrophilic part of HFBI also has absorption preference of polar molecules over non-polar molecules.

Furthermore, we investigated the influence of pH fluctuations on the sensor performance. In many practical circumstances, the water vapor to be detected can be acidic or alkalic, which may dramatically degrade the performance of the humidity sensor. However, as the HFBI is very stable in acid and alkali solutions, it efficient shield the pH influence on the HFBI wrapped rGO sensor. To demonstrate this, we exposed the sensor to the water vapors which were bubbled out through the HCl or KOH solutions with pH values ranging from 2 to 12 and the RH value was set at 20%. As shown in Fig. 4b, the responses of the sensor to various pH values were almost the same: similar rising/falling time and a variation within 10% of the maximum equilibrium values. This result demonstrates that the HFBI can successfully shield the sensor from pH fluctuation, a property that is highly favored for applications in many bio/chemical sensing areas.

Finally, it is worth noting that the resistance of HFBI wrapped rGO sensor increases, instead of decreasing, under the exposure to water molecules which is opposite to the previously reported result of GO, partially reduced GO and graphene/polymer nanocomposites sensors [43–46], suggesting a different sensing mechanism of the HFBI wrapped rGO sensor. Water molecules usually result in two effects that cause the change of resistance when they are adsorbed by GO/rGO sensors: 1) water vapor behaves like an electron acceptor, which causing further p-doping in GO/rGO comparing to its intrinsic status before absorbing water molecules, causing either the decrease or increase of the resistance which is determined by the intrinsic doping of the material [47–49]; 2) the absorbed water molecules can expand interlayer spacing leading to

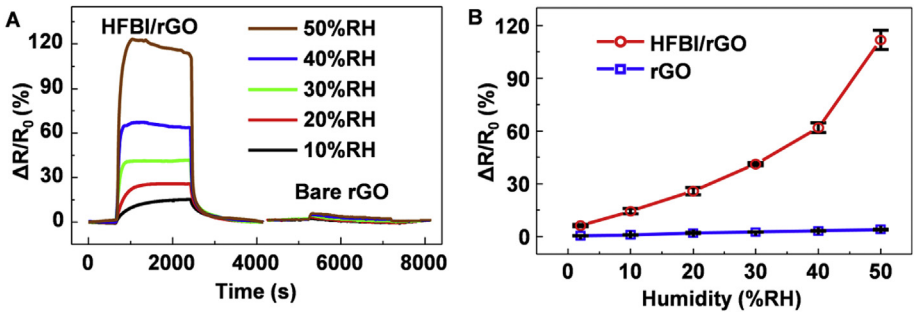

Fig. 3. Sensing responses comparison between the HFBI wrapped rGO and bare rGO to water molecules. (a) Real-time responses of HFBI wrapped rGO sensor (left) and bare rGO sensor (right) to RH ranging from 2% to 50%, respectively. (b) Relative resistance change upon the exposure to water molecules at the maximum equilibrium vs. RH values. Red and blue lines represent HFBI wrapped rGO sensor and bare rGO sensor, respectively. (A colour version of this figure can be viewed online.)

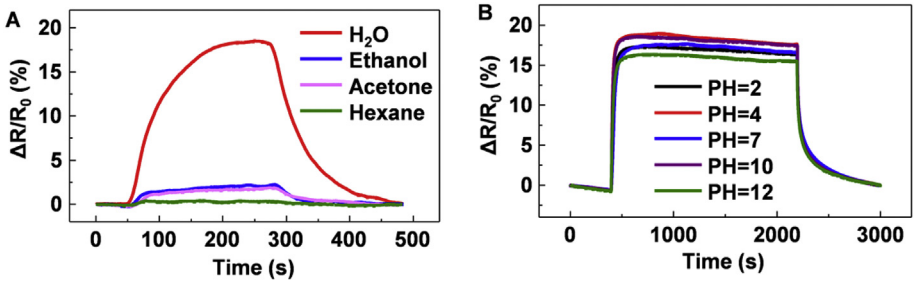

Fig. 4. Selectivity of the HFBI wrapped rGO sensor. (a) Real-time responses of HFBI wrapped rGO sensor to various vapor analytes. (b) Real-time responses of HFBI wrapped rGO sensor to water vapors bubbling from different solutions with pH values ranging from 2 to 12. (A colour version of this figure can be viewed online.)

the increase of the interlayer resistance [50,51]. GO/rGO is well known to be p-type semiconductor, and therefore, the resistance of bare GO, which has very few carriers but a large number of functional groups at the surface, decreases when exposed to water vapor, because the increase of p doping induced by water molecules plays a more significant role than the increase of interlayer spacing. On the contrary, rGO has very few functional groups, resulting in limited absorption of water molecules, and therefore either the carrier donation or interlayer spacing is not significant, leading to the minor resistance change with a sensor based on bare rGO. In the case of HFBI wrapped rGO flakes, the HFBI increases the absorption of the water molecules, resulting in the expansion of the interlayer space between HFBI wrapped rGO flakes. However, the protein layer wrapped outside the rGO flake prevents the water molecules from reaching the basal plane of rGO [52], and thus minimizes the water molecule induced p-doping effect. As a result, the interlayer spacing effect dominates and causes the increase of the resistance of HFBI wrapped rGO sensor when exposed to water vapor.

Compared to other liquid phase exfoliation and functionalization methods, the hydrophobin approach offers many unique advantages. First of all, it accomplishes the exfoliation and functionalization simultaneously within one-step. A one-step approach not only significantly simplifies the fabrication process but also avoids potential impurity or pollution to the final product which is quite common in multi-step processes. Second, hydrophobin functionalization enhances the molecules adsorption on the surface. The bare surface of 2DLM, graphene for example, has little attractions to bio/chemical molecules, resulting in limited response for adsorption based applications [9,17,53,54]. On the contrary, as the 2DLM is wrapped with hydrophobin, the adsorption capability is greatly improved due to the roughened surface of hydrophobin [55,56]. Third, hydrophobin forms an ultra-high density and ordered monolayer to shield the 2DLM from the ambient environment, so that the bio-nanocomposites can preserve the original properties of 2DLM and stabilize the device performance from charge fluctuation in background environment [55]. This also helps protect some unstable 2DLM material, such as black phosphorus from degradation. At last, hydrophobin improves the biocompatibility of the 2DLM which broadens its applications in multiple fields, such as in vivo bio-sensing, bio-imaging, drug delivery, displaying and multi-gas detection.

4. Conclusion

In conclusion, we have demonstrated a new method to mass exfoliate and functionalize 2DLM by hydrophobin HFBI within a single step which bridges 2DLM with life science field for vast potential applications. The hydrophobin can not only successfully exfoliate mono-/few-layered 2DLM with comparable sizes and thicknesses with other liquid exfoliation methods, but also spontaneously functionalize the exfoliated 2DLM by wrapping its entire surface with a dense and ordered hydrophobin monolayer. The resultant bio-nanocomposites of hydrophobin wrapped 2DLM possess augmented molecule adsorption capability and biocompatibility which enable numerous practical applications in various areas including chemistry, biology, medical care, and environmental protection. An exemplary application of the HFBI exfoliated and functionalized rGO sensor is developed for water molecular sensing. The sensor exhibits an improved detection limit of 2% RH and reasonable dynamic range up to 50%, in comparison with other GO/rGO humidity sensors. It also showed great selectivity to water molecules over VOCs and long term stability under environments with extreme pH values, demonstrating its promising sensing potential.

For future work, further study will be focused on the HFBI exfoliation method to fabricate mono/few layer 2DLM sheet with accurately controlled size and thickness. Meanwhile, other applications of the HFBI/2DLM bio-nanocomposites will be explored,

such in vivo bio-sensing, bio-imaging and drug delivery.

Acknowledgments

The research is supported by the National Science Foundation of China (No. 21405109 and No. 61501320), the Natural Science Foundation of Tianjin, China (No. 14JCYBJC43500) and the State Key Laboratory of Medicinal Chemical Biology, China (No. 201503015).

Appendix A. Supplementary data

Supplementary data related to this article can be found at http://dx.doi.org/10.1016/j.carbon.2017.02.052.

References

[1] K.S. Novoselov, A.K. Geim, S.V. Morozov, D. Jiang, Y. Zhang, S.V. Dubonos, et al., Electric field effect in atomically thin carbon films, Science 306 (2004) 666–669.
[2] J. Xu, Z. Tan, W. Zeng, G. Chen, S. Wu, Y. Zhao, et al., A hierarchical carbon derived from sponge-templated activation of graphene oxide for high-performance supercapacitor electrodes, Adv. Mater 28 (2016) 5222–5228.
[3] M. Xu, T. Liang, M. Shi, H. Chen, Graphene-like two-dimensional materials, Chem. Rev. 113 (2013) 3766–3798.
[4] C.-H. Liu, Y.-C. Chang, T.B. Norris, Z. Zhong, Extracting the complex optical conductivity of mono-and bilayer graphene by ellipsometry, Appl. Phys. Lett. 104 (2014) 261909.
[5] J.N. Coleman, M. Lotya, A. O'Neill, S.D. Bergin, P.J. King, U. Khan, et al., Two-dimensional nanosheets produced by liquid exfoliation of layered materials, Science 331 (2011) 568–571.
[6] Y. Hernandez, V. Nicolosi, M. Lotya, F.M. Blighe, Z. Sun, S. De, et al., High-yield production of graphene by liquid-phase exfoliation of graphite, Nat. Nanotechnol. 3 (2008) 563–568.
[7] J. Kang, J.D. Wood, S.A. Wells, J.H. Lee, X. Liu, K.S. Chen, et al., Solvent exfoliation of electronic-grade, two-dimensional black phosphorus, ACS Nano 9 (2015) 3596–3604.
[8] F. Wang, Z. Wang, Q. Wang, F. Wang, L. Yin, K. Xu, et al., Synthesis, properties and applications of 2D non-graphene materials, Nanotechnology 26 (2015) 292001.
[9] V. Georgakilas, M. Otyepka, A.B. Bourlinos, V. Chandra, N. Kim, K.C. Kemp, et al., Covalent modification of exfoliated fluorographite with nitrogen functionalities, J. Mater. Chem. C 3 (2015) 7627–7631.
[10] T. Ramanathan, A.A. Abdala, S. Stankovich, D.A. Dikin, M. Herrera-Alonso, R.D. Piner, et al., Functionalized graphene sheets for polymer nanocomposites, Nat. Nanotechnol. 3 (2008) 327–331.
[11] K.N. Kudin, B. Ozbas, H.C. Schniepp, R.K. Prud'homme, I.A. Aksay, R. Car, Raman spectra of graphite oxide and functionalized graphene sheets, Nano Lett. 8 (2008) 36–41.
[12] C.X. Guo, X.T. Zheng, Z.S. Lu, X.W. Lou, C.M. Li, Biointerface by cell growth on layered graphene-artificial peroxidase-protein nanostructure for in situ quantitative molecular detection, Adv. Mater 22 (2010) 5164–5167.
[13] R. Muszynski, B. Seger, P.V. Kamat, Decorating graphene sheets with gold nanoparticles, J. Phys. Chem. C 112 (2008) 5263–5266.
[14] P.T. Yin, S. Shah, M. Chhowalla, K.B. Lee, Design, synthesis, and characterization of graphene–nanoparticle hybrid materials for bioapplications, Chem. Rev. 115 (2015) 2483–2531.
[15] S. Niyogi, E. Bekyarova, M.E. Itkis, J.L. Mcwilliams, M.A. Hamon, R.C. Haddon, et al., Solution properties of graphite and graphene, Chem. Soc. 128 (2006) 7720–7721.
[16] T. Kuila, S. Bose, A.K. Mishra, P. Khanra, N.H. Kim, J.H. Lee, et al., Chemical functionalization of graphene and its applications, Mater. Sci. 57 (2012) 1061–1105.
[17] M. Yi, Z. Shen, A review on mechanical exfoliation for the scalable production of graphene, J. Mater. Chem. A 3 (2015) 11700–11715.
[18] Y. Zhang, S. Liu, L. Wang, X. Qin, J. Tian, W. Lu, et al., One-pot green synthesis of Ag nanoparticles-graphene nanocomposites and their applications in SERS, H2O2, and glucose sensing, RSC Adv. 2 (2012) 538–545.
[19] S. Stankovich, D.A. Dikin, R.D. Piner, K.A. Kohlhaas, A. Kleinhammes, Y. Jia, et al., Synthesis of graphene-based nanosheets via chemical reduction of exfoliated graphite oxide, Carbon 45 (2007) 1558–1565.
[20] H.C. Schniepp, J.L. Li, M.J. McAllister, H. Sai, M. Herrera-Alonson, D.H. Adamson, et al., Functionalized single graphene sheets derived from splitting graphite oxide, J. Phys. Chem. B 110 (2006) 8535–8539.
[21] H. Bai, Y. Xu, L. Zhao, C. Li, G. Shi, Non-covalent functionalization of graphene sheets by sulfonated polyaniline, Chem. Commun. 4 (2009) 1667–1669.
[22] P. Laaksonen, M. Kainlauri, T. Laaksonen, A. Shchepetov, H. Jiang, J. Ahopelto, et al., Interfacial engineering by proteins: exfoliation and functionalization of graphene by hydrophobins, Angew. Chem. - Int. Ed. 49 (2010) 4946–4949.
[23] M. Pykal, K. Safarova, K. Machalova Siskova, P. Jurecka, A.B. Bourlinos, R. Zboril, et al., Lipid enhanced exfoliation for production of graphene nanosheets, J. Phys. Chem. C 117 (2013) 11800–11803.
[24] Y. Lu, B.R. Goldsmith, N.J. Kybert, A.T.C. Johnson, DNA-decorated graphene chemical sensors, Appl. Phys. Lett. 97 (2010) 083107.
[25] M. Linder, K. Selber, T. Nakari-Setälä, M. Qiao, M.R. Kula, M. Penttilä, The Hydrophobins HFBI and HFBII from Trichoderma reesei Showing Efficient Interactions with nonionic surfactants in aqueous two-phase systems, Biomacromolecules 2 (2001) 511–517.
[26] J. Hakanpää, A. Paananen, S. Askolin, T. Nakari-Setälä, T. Parkkinen, M. Penttilä, et al., Atomic resolution structure of the HFBII hydrophobin, a self-assembling amphiphile, J. Biol. Chem. 279 (2004) 534–539.
[27] J. Hakanpää, G.R. Szilvay, H. Kaljunen, M. Maksimainen, M. Linder, J. Rouvinen, Two crystal structures of trichoderma reesei hydrophobin HFBI—the structure of a protein amphiphile with and without detergent interaction, Protein Sci. 15 (2006) 2129–2140.
[28] G.R. Szilvay, A. Paananen, K. Laurikainen, E. Vuorimaa, H. Lemmetyinen, J. Peltonen, et al., Self-assembled hydrophobin protein films at the air-water interface: structural analysis and molecular engineering, Biochemistry 46 (2007) 2345–2354.
[29] H.A. Wösten, F.H. Schuren, J.G. Wessels, Interfacial self-assembly of a hydrophobin into an amphipathic protein membrane mediates fungal attachment to hydrophobic surfaces, EMBO J. 13 (1994) 5848.
[30] K.M. Bromley, R.J. Morris, L. Hobley, G. Brandani, R.M.C. Gillespie, M. McCluskey, et al., Interfacial self-assembly of a bacterial hydrophobin, Proc. Natl. Acad. Sci. 112 (2015) 5419–5424.
[31] S. Stankovich, R.D. Piner, S.T. Nguyen, R.S. Ruoff, Synthesis and exfoliation of isocyanate-treated graphene oxide nanoplatelets, Carbon 44 (2006) 3342–3347.
[32] Z. Wang, Y. Wang, Y. Huang, S. Li, S. Feng, H. Xu, et al., Characterization and application of hydrophobin-dispersed multi-walled carbon nanotubes, Carbon 48 (2010) 2890–2898.
[33] L. Fan, C. Luo, M. Sun, H. Qiu, Synthesis of graphene oxide decorated with magnetic cyclodextrin for fast chromium removal, J. Mater. Chem. 22 (2012) 24577–24583.
[34] M.L. de Vocht, K. Scholtmeijer, E.W. van der Vegte, O.M. de Vries, N. Sonveaux, H.A. Wosten, et al., Structural characterization of the hydrophobin SC3, as a monomer and after self-assembly at hydrophobic/hydrophilic interfaces, Biophys. J. 74 (1998) 2059–2068.
[35] A.C. Ferrari, J.C. Meyer, V. Scardaci, C. Casiraghi, M. Lazzeri, F. Mauri, et al., Raman spectrum of graphene and graphene layers, Phys. Rev. Lett. 97 (2006) 187401.
[36] X. Cui, C. Zhang, R. Hao, Y. Hou, Liquid-phase exfoliation, functionalization and applications of graphene, Nanoscale 3 (2011) 2118–2126.
[37] A. Eckmann, A. Felten, A. Mishchenko, L. Britnell, R. Krupke, K.S. Novoselov, et al., Probing the nature of defects in graphene by Raman spectroscopy, Nano Lett. 12 (2012) 3925–3930.
[38] K.R. Paton, E. Varrla, C. Backes, R.J. Smith, U. Khan, A. O'Neill, et al., Scalable production of large quantities of defect-free few-layer graphene by shear exfoliation in liquids, Nat. Mater 13 (2014) 624–630.
[39] A. Ghosh, D.J. Late, L.S. Panchakarla, a Govindaraj, C.N.R. Rao, NO2 and humidity sensing characteristics of few-layer graphenes, J. Exp. Nanosci. 4 (2009) 313–322.
[40] D. Zhang, J. Tong, B. Xia, Humidity-sensing properties of chemically reduced graphene oxide/polymer nanocomposite film sensor based on layer-by-layer nano self-assembly, Sensors Actuators, B Chem. 197 (2014) 66–72.
[41] P.-G. Su, C.-F. Chiou, Electrical and humidity-sensing properties of reduced graphene oxide thin film fabricated by layer-by-layer with covalent anchoring on flexible substrate, Sensors Actuators B Chem. 200 (2014) 9–18.
[42] A.D. Smith, K. Elgammal, F. Niklaus, A. Delin, A.C. Fischer, S. Vaziri, F. Forsberg, M. Råsander, H. Hugosson, L. Bergqvist, S. Schröder, S. Kataria, M. Östling, M.C. Lemme, Resistive graphene humidity sensors with rapid and direct electrical readout, Nanoscale 7 (2015) 19099–19109.
[43] S. Borini, R. White, D. Wei, M. Astley, S. Haque, E. Spigone, et al., Ultrafast graphene oxide humidity sensors, ACS Nano 7 (2013) 11166–11171.
[44] S. Ali, A. Hassan, G. Hassan, J. Bae, C.H. Lee, All-printed humidity sensor based on gmethyl-red/methyl-red composite with high sensitivity, Carbon 105 (2016) 23–32.
[45] W. Yuan, A. Liu, L. Huang, C. Li, G. Shi, High-performance NO_2 Sensors based on chemically modified graphene, Adv. Mater. 25 (2013) 766–771.
[46] W. De Lin, H.M. Chang, R.J. Wu, Applied novel sensing material graphene/polypyrrole for humidity sensor, Sens. Actuators B Chem. 181 (2013) 326–331.
[47] W. Yuan, G. Shi, Graphene-based gas sensors, J. Mater. Chem. A 1 (2013) 10078–10091.
[48] J. Kong, N.R. Franklin, C.W. Zhou, M.G. Chaplin, Sh Peng, K. Cho, et al., Nanotube molecular wires as chemical sensors, Science 287 (2000) 622–625.
[49] K.S. Kim, Y. Zhao, H. Jang, S.Y. Lee, J.M. Kim, J.-H. Ahn, et al., Large-scale pattern growth of graphene films for stretchable transparent electrodes, Nature 457 (2009) 706–710.
[50] Y. Yao, X. Chen, H. Guo, Z. Wu, Graphene oxide thin film coated quartz crystal microbalance for humidity detection, Appl. Surf. Sci. 257 (2011) 7778–7782.
[51] H.-W. Yu, H.K. Kim, T. Kim, K.M. Bae, S.M. Seo, J.-M. Kim, et al., Self-powered humidity sensor based on graphene oxide composite film intercalated by poly (sodium 4-styrenesulfonate), ACS Appl. Mater. Interfaces 6 (2014) 8320–8326.
[52] Y. Dan, Y. Lu, N.J. Kybert, Z. Luo, A.T.C. Johnson, Intrinsic response of graphene

vapor sensors, Nano Lett. 9 (2009) 1472–1475.
[53] Y. Shao, J. Wang, H. Wu, J. Liu, I.A. Aksay, Y. Lin, Graphene based electrochemical sensors and biosensors: a review, Electroanalysis 22 (2010) 1027–1036.
[54] V.C. Sanchez, A. Jachak, R.H. Hurt, a B. Kane, Biological interactions of graphene-family nanomaterials: an interdisciplinary review, Chem. Res. Toxicol. 25 (2012) 15–34.
[55] M.B. Linder, G.R. Szilvay, T. Nakari-Setälä, M.E. Penttilä, Hydrophobins: the protein-amphiphiles of filamentous fungi, FEMS Microbiol. Rev. 29 (2005) 877–896.
[56] K. Scholtmeijer, J.G.H. Wessels, H.A.B. Wösten, Fungal hydrophobins in medical and technical applications, Appl. Microbiol. Biotechnol. 56 (2001) 1–8.